SUPPLEMENTARY MATERIALS to "THE FATE OF BARS IN BRAIDED RIVERS"

Authors: Alpheus, S.[1] & Hajek, E.[1]

Author affiliations: 1- Department of Geosciences, The Pennsylvania State University, University Park, PA 16802

Corresponding Author: Safiya Alpheus (safiyaalpheus1@gmail.com)

Contents:

SUPPLEMENTAL METHODS

Model Setup

The grid dimensions and initial parameters defined in the model are defined in table S1. In the model we sampled from a normal distribution of discharges where mean discharge was 100 m^3/s and allowed to vary randomly between 99.5 and 100.5 m^3/s every 12 hours to create noise in the model that retained the dynamics necessary for continuous bar growth and decay. Similar approaches have been carried out in numerical and experimental studies (Van Dijk et al., 2012; Schuurman et al., 2013), and in our set up, the maximum discharge perturbation accounts for 1.33% of the mean discharge—at the scale of noise, rather than a forcing.

Table S1: Key model input parameters and defined variables used in NAYS2DH braided river simulation

Model input parameter	Unit	Value
Grid cell width x length	m	4 x 10
Initial grid width x length	m	100 x 10000
Slope	n.d.	0.00137
Grain size	mm	0.31
Manning's bed roughness coefficient	$m^{1/3}/s$	0.012
Discharge, Q	m^3/s	100
MorFac	n.d.*	25
Sediment transport predictor		Ashida & Michiue (1972)[1]
Perturbation max. initial bed level	m	.01
Perturbation period of Q	hours	12
SD of Q Perturbation	m^3/s	0.5
Hydrodynamic timestep	sec	0.1
Morphodynamic timestep	sec	2.5
Bank height	m	2
Bank angle of repose	°	17
Outlet conditions	n/a	Uniform flow

*(n.d. = non-dimensional)

1- Bed load transport estimated using Ashida and Michiue (1972) predictor for sediment transport described in the NAYS2DH Solver Manual (Section II.5.2, p.12-13 Shimizu et al., 2011). As described in the manual, this predictor is best for mixed grain sizes and considers local bed slope effects in both the transverse and streamwise direction when estimating bed load transport.

Pseudofacies Calculation

The distribution of bedforms was modelled in the model domain using the modelled flow depth and velocity outputs and the bedform stability diagram (Figure S1.1) proposed by Van den berg and van Gelder (1993). We used this parameterization as it was developed for field applications in fine sand and silt-rich systems, and requires only flow depth and velocity, and grain size inputs—parameters and measurements attainable in field outcrops. In the model, bed mobility is defined as follows:

$$\theta = \frac{\rho \overline{u}^2}{(\rho_s - \rho) C'^2 D_{50}} \qquad (1)$$

Where ρ = fluid density in kg/m^3, ρs = sediment density (kg/m^3), $\overline{u}$ = depth averaged velocity [m/s], D_{50} = median grain size (m) and C' is defined as:

$$C' = 18 \log\left(\frac{4h}{D_{90}}\right) \qquad (2)$$

Where h = flow depth (m) and D_{90} = ninetieth percentile grain size.

We use the following facies cut-offs (Table S2) in the model stratigraphy to represent shear-stress gradients that produce different sedimentary structures in the field. These categories are used to indicate different suites of sedimentary structures and channel-deposit facies present in fluvial deposits; the specific cut-offs used here are representative and, in natural systems, would differ based on specific grain sizes and flow conditions.

Table S2: Upper and Lower Bar facies and their defining bedform definitions and modified mobility parameter, θ, ranges

	Defining bedforms	θ range
Upper Bar Facies (UB)	No Movement (NM)	NM: <0.01
	Lower stage plane bedding (LP)	LP: 0.01-0.025
Lower Bar Facies (LB)	Ripples (R)	R: 0.025-0.15
	Dunes (D)	D: 0.15-0.35
	Upper stage plane bedding (UP)	UP: 0.35-1.5

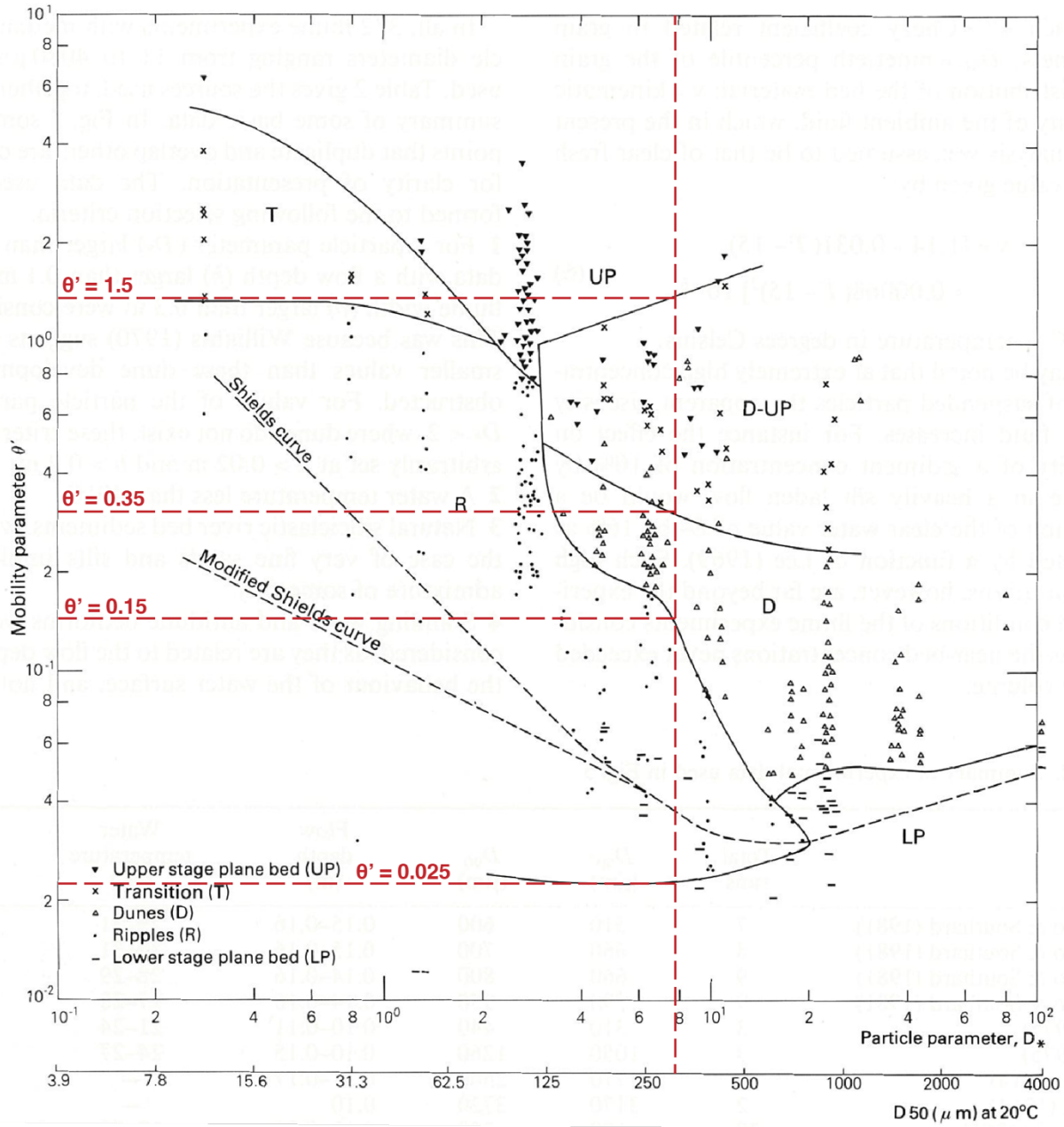

Figure S1: (modified from Van Den Berg and Van Gelder (1993): Bedform stability relationship computed relative to grain mobility parameter and grain size. Red dashed lines highlight locations of mobility parameters estimated for different pseudofacies in braided river model used in this manuscript: where theta = 0.025, 0.15, 0.35, 1.5 represents the upper limits of stability of lower stage plane bedding, ripples, dunes, and dunes-upper stage plane bedding respectively.

Bar Turnover Timescale

Bar package turnover timescale was estimated as the amount of time required to displace a bar in the downstream direction, based on the unit sediment flux. We estimated the turnover timescale adapting the equation for bedform turnover timescale following Martin and Jerolmack (2013), Myrow (2018) and Leary and Ganti (2020) for bars in downstream sections:

$$T_T = \frac{\beta \lambda h_B}{q_b} \qquad (3)$$

Where β = 0.5—a shape factor, here we assumed a triangular bar shape; λ = bar length—the distance between successive minima on the bed used to define the base of the bar; h_B = bar height—the perpendicular height of the bar; and q_b = cross-section averaged unit sediment flux recorded at the head of the bar.

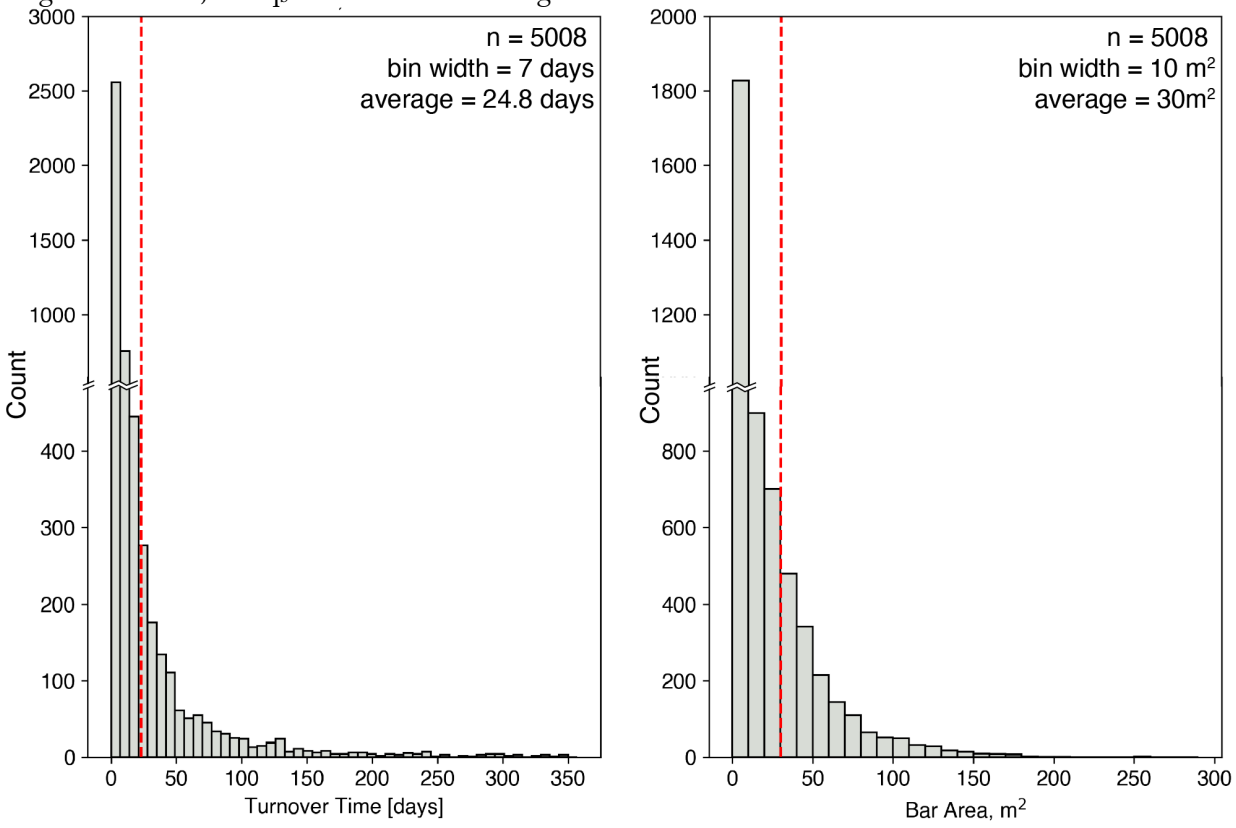

Figure S2: Distribution of bar turnover timescales (left) and estimated bar area (right; assuming triangular bar shape) for bars formed along a 1km long transect along the center of the model grid from 3000m-4000m downstream. Red dashed lines in both plots indicate the average bar turnover time (24.8 days) and bar area (30m^2) for the model run.

Data Processing & Bar Mapping

Data Processing

Each solution to the model bed is output as a .csv file at pre-determined output intervals. These outputs were combined and stacked to conduct the stratigraphic mapping in this manuscript.

To build each stratigraphic cross-section from stacked channel floor topography, channel topography was repositioned from the model co-ordinate reference grid (NAYS2DH curvilinear grid system [I, J]) to a geographic grid (2D cartesian grid [X, Y]). The data (bed elevation, shear stress, flow depth, flow velocity, bedload flux) at each cross-section location and each timestep were interpolated using a cubic interpolation with 1m spacing which provided a uniformly dataset from which the bed elevation outputs could be combined and used to build the stratigraphic cross-sections.

To build the stratigraphic cross-sections: at each cross-section location, per output timestep [T_n], bed elevation at every location along the cross-section was cross referenced against the preceding elevations [T_0, T_1, …, T_{n-1}], and the bed elevations of all preceding timesteps were reset to the elevation at time T if the elevation exceeded the elevation at time T (i.e. erosion of the bed). In the case that elevation at time T was larger than the elevation at the same location for the preceding timesteps, the new layer of the bed was deposited (bed elevation at time T).

Bar mapping for each cross section was carried out using a script written with the intent to automate as much of the mapping process as possible, which expedited workflow and the maximized the amount of data that could be collected describing the sections and bar packages. Due to this emphasis, ambiguities, or misattribution of the timing of the final erosion surface contribute to little gaps in the mapping of the bars in the cross sections, or the process can occasionally miss final scour surfaces or minor erosion/hiatal surfaces, omitting some minor portions of bars from the analysis.

The semi-automated bar mapping script plots the cross-section in question and by user selection (clicking) of the left and right edges and upper and lower bounding surfaces of a bar package, the algorithm searches the cross-section for the best-fit spatial and temporal solution for the LeftEdge and RightEdge and StartTime and EndTime indices of the bar package that define the sub-section of greater cross-section's master NumPy array over which the data relevant to the bar package mapped is stored. The code then crops the master array to the dimensions of the bar package and extracts the desired attributes and statistics that describe the bar package to a .csv file for each cross-section. The .csv data were then compiled to produce AH2023_BarLibrary.xlsx that describes all bar packages mapped in the study.

DATA AVAILABILITY

Video of model planform evolution

The video of the complete model run is available at https://youtu.be/urO67fodE5I and for download in the ScholarSphere repository Dataset for "The Fate of Bars in Braided Rivers".

Mapped cross-sections and scripts for analysis

Several python scripts have been used to process the model results and perform analyses on the data. The scripts used to process the NAYS2DH model outputs are hosted in the GitHub repository https://github.com/salpheus/BarPreservation.

The repository [https://scholarsphere.psu.edu/resources/d20f3886-158f-40de-9db9-9c7b82e4719] hosts the following data products associated with this manuscript:

- All .csv files output for the duration of the model run (agubh2-10km.zip)
- Composite arrays of the each timestep output of bed elevation, the processed stratigraphy, local flow depth, bed shear stress, flow velocity and modified mobility parameter (Van Den Berg and Van Gelder, 1993) for each mapped cross section (in the cross-stream direction; AH_Bar_Cross-Sections.zip)
- Scripts to replot each cross-section from the above composite files (AH_Replot_Sections_Supplement.ipynb)
- A compilation of the 33 cross-sections mapped in this study (AH2023-Bar-Library.pdf)
- All measurements collected for each bar package mapped in each cross-section (AH2023_BarLibrary.xlsx)

Details and measurements for the bars mapped are recorded in the file AH2023-BarLibrary.xlsx. For each mapped bar package, we include the following:

1. **BarName:** unique identifier for each bar.
    a. *Naming convention: [section location]-[preservation flag]-[unique ID]*
2. **ArrayName:** unique name of the array
3. **ILoc:** grid location of the cross-section in cellular co-ordinates (measured in downstream direction). To convert from grid cell location to XY location, multiply by 10 (1 cell = 10m long)
4. **PreservChar:** Flag that describes preservation character of package where FP = Fully preserved, PP = Partially Preserved and TR = Truncated
5. **StartTime:** Age of basal erosion/downlap surface
6. **EndTime:** Age of upper bounding surface
7. **ElapsedTime:** Length of deposition (difference between StartTime and EndTime)
8. **LeftEdge:** Location of left edge of bar package (measured relative to the leftmost edge of the stratigraphic cross-section at *'Iloc'*)
9. **RightEdge:** Location of the right edge of the bar package (measured relative to the leftmost edge of the stratigraphic cross section at *'Iloc'*)
10. **BarWidth:** Maximum width of the bar package (difference between LeftEdge and RightEdge) [m]
11. **BarHeight:** Maximum height of the bar package (height between minimum and maximum bar topography) [m]
12. **BarAspect:** Bar Width:Height ratio
13. **BarArea:** Area of bar package [m^2]

14. **SectionArea:** Area of stratigraphic cross-section at *'Iloc'* [m^2]
15. **ChannelProp:** Area of bar package relative to area of cross section at *'Iloc'*
16. **MaxClinoHt:** Maximum height of clinothems within the bar package
17. **MeanClinoHt:** Average height of clinothems within the bar package
18. **MeanClinoWt**: Average width of clinothems within the bar package
19. **MaxFlowDepth**: Mean local flow depth during deposition of bar package (i.e. in channel domain at Iloc, between LeftEdge and RightEdge during StartTime and EndTime)
20. **MeanFlowDepth**: Maximum local flow depth during deposition of bar package (i.e. in channel domain at Iloc, between LeftEdge and RightEdge during StartTime and EndTime)
21. **MeanShear:** Mean local shear stress [N/m^2] during deposition of bar package (i.e. in channel domain at Iloc, between LeftEdge and RightEdge during StartTime and EndTime)
22. **MeanVelocity:** Mean local flow velocity [m/s] during deposition of bar package (i.e. in channel domain at Iloc, between LeftEdge and RightEdge during StartTime and EndTime)
23. BarHeight/MaxFlowDepth: Ratio between bar height and maximum local flow depth
24. MaxClino/MaxFlowDepth: Ratio between maximum clinothem height within the bar package and the maximum local flow depth
25. **BL/CL:** Ratio of bar length maximum clinothem length
26. GrowthR8: Bulk average sedimentation rate across bar package calculated by dividing BarArea by ElapsedTime
27. UBar: Proportion of bar package area occupied by Upper Bar pseudo-facies (No-Movement and Lower Stage Plane Bedding)
28. **MeanAge:** Mean age of clinothem surfaces within bar package

ADDITIONAL TESTS & RESULTS

Table S3: Change in percentage (%) abundance of pseudo-structures from the bed to stratigraphy in 33 mapped cross-sections across the model domain. Locations of mapped sections shown in Figure 2A.

Pseudo-structure	% bed area occupied from t=65 to end of run	% of stratigraphic area occupied	Proportion Change $\left(\frac{\%_{Strat}}{\%_{Bed}}\right)$
No Movement	19.6	8.4	0.42
Lower Stage Plane Bedding	11.5	8.5	0.73
Ripples	44.5	43.3	0.97
Dunes	15.7	21.2	1.35
Dunes-Upper Stage Plane Bedding	8.7	17.8	2.0
Upper Stage Plane Bedding	0.1	0.7	7.0

Relationship between channel morphodynamics and preservation

To quantitatively test the relationship between widening rate, Entropic Braiding Index (eBI) and bar package preservation, we performed least-squares regressions between (1) the mean and median widening rate and the mean and median proportion of cross-section area occupied by preserved (fully and partially preserved) packages in each mapped cross-section (Figure S3); and (2) the mean and median eBI and the mean and median proportion of cross-section area occupied by preserved (fully and partially preserved) packages in each mapped cross-section (Figure S4). Both tests yielded linear regressions with weak R^2 values (-0.14 and -0.38 for widening rates) and (-0.04 and -0.05 for eBI), further supporting the observation that there is no relationship between widening rate, braiding intensity, and bar package preservation in braided rivers.

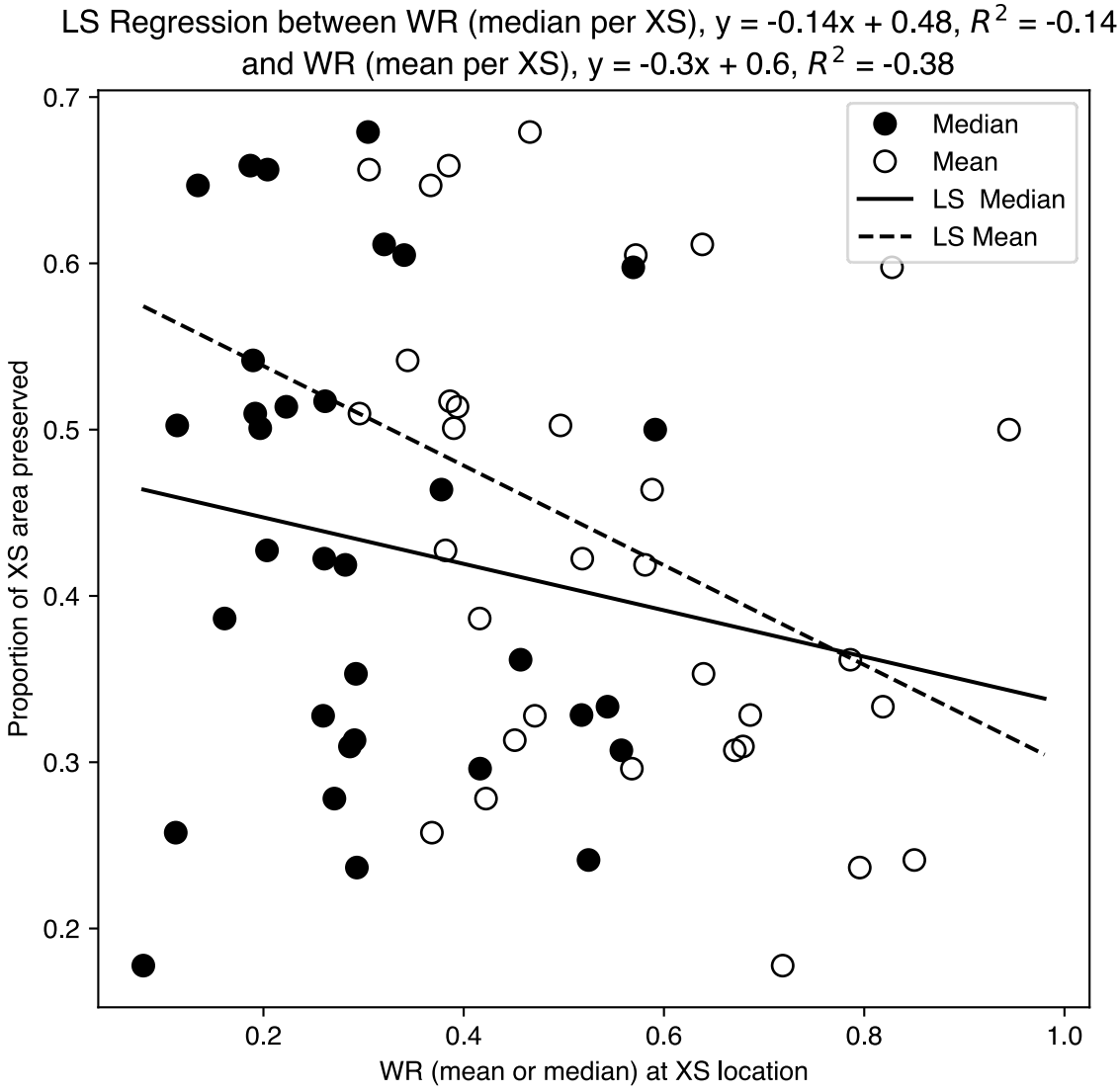

Figure S3 : Least-squares regression (LS) of median and mean widening rate (WR) and preserved cross-section (XS) area at each mapped cross section area.

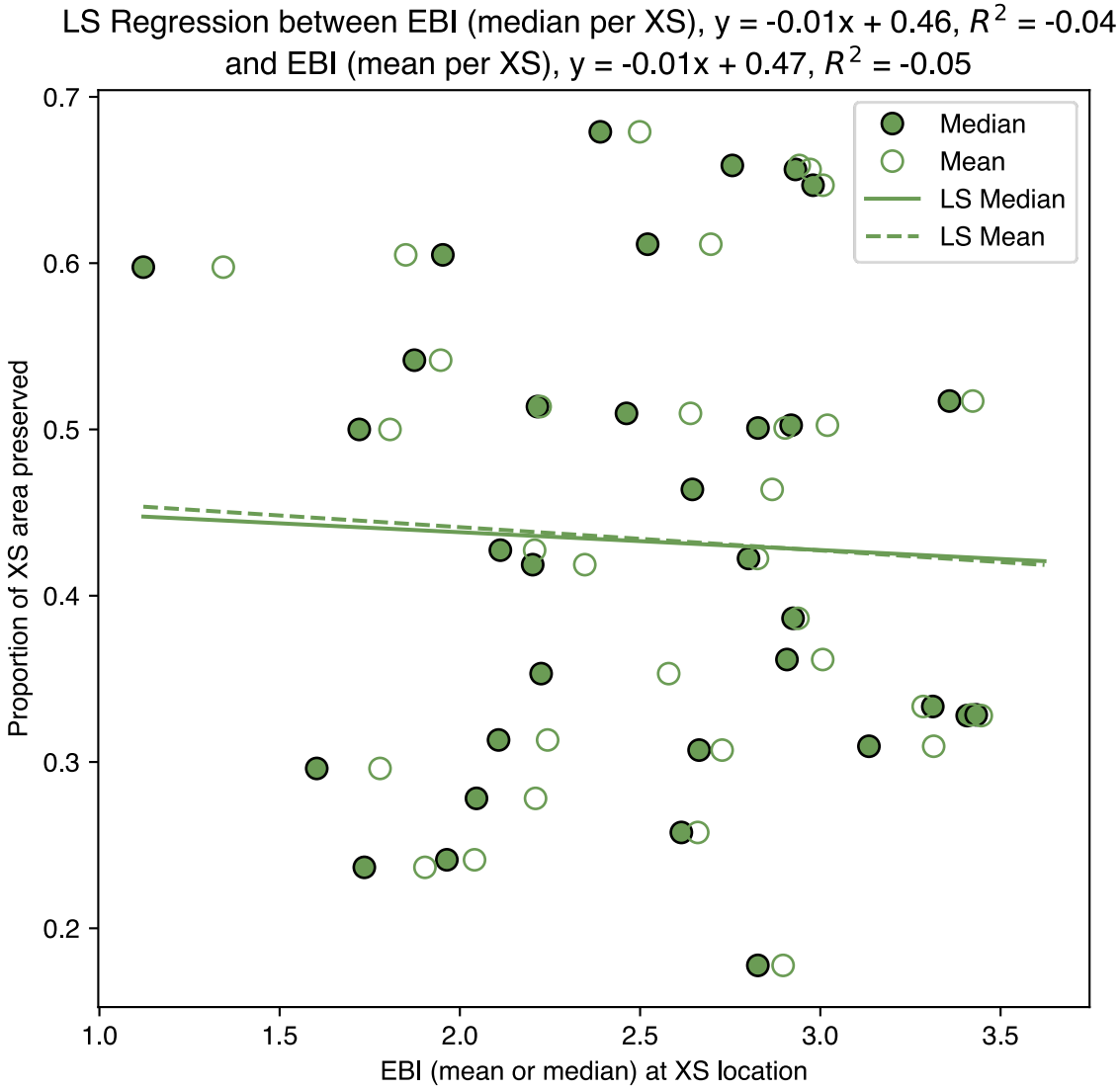

Figure S4: Least-squares regression (LS) of median and mean Entropic Braiding Index (eBI) and preserved cross-section (XS) area at each mapped cross section area.

Additional measurements in bar package and clinoform geometry, facies, and hydraulic relationships

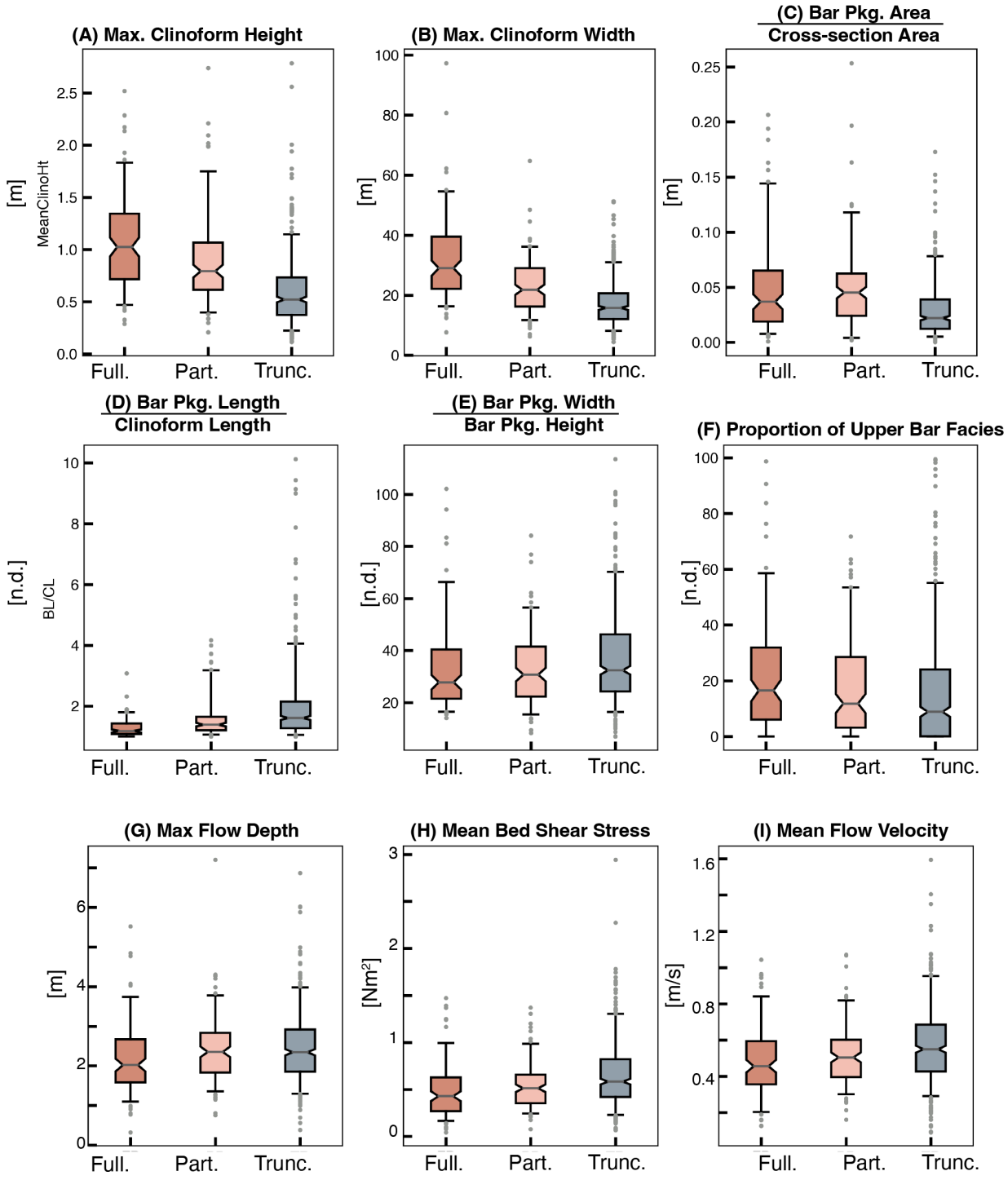

Figure S5: Geometric characteristics (A-B), scaling relationships (C-E), the proportion (%) of upper bar facies (F), and hydraulic characteristics (G-I) of fully, partially preserved, and truncated bar packages and clinoform surfaces mapped in the model domain.

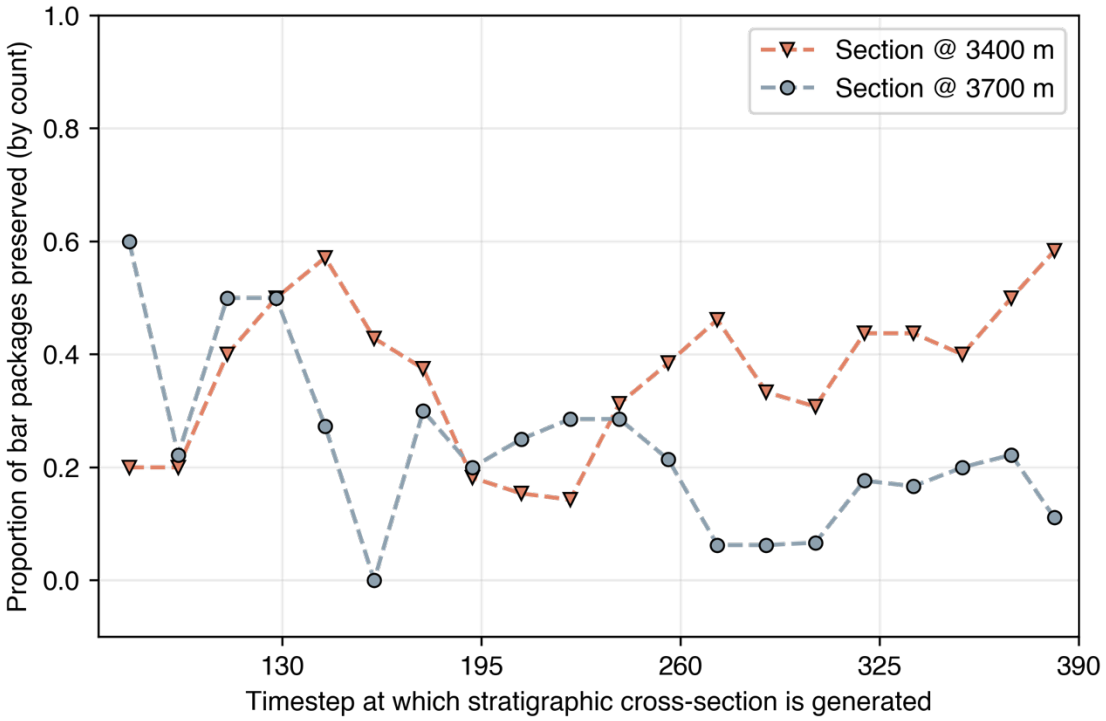

Figure S6: Bar preservation in the model stratigraphy at section A (@3400 m) and section B (@3700 m), if cross-sections were constructed using topography generated at different timesteps (i.e. simulating termination of the model run at different timesteps). Locations of section A and B shown in Figures 2 and 5 in manuscript.

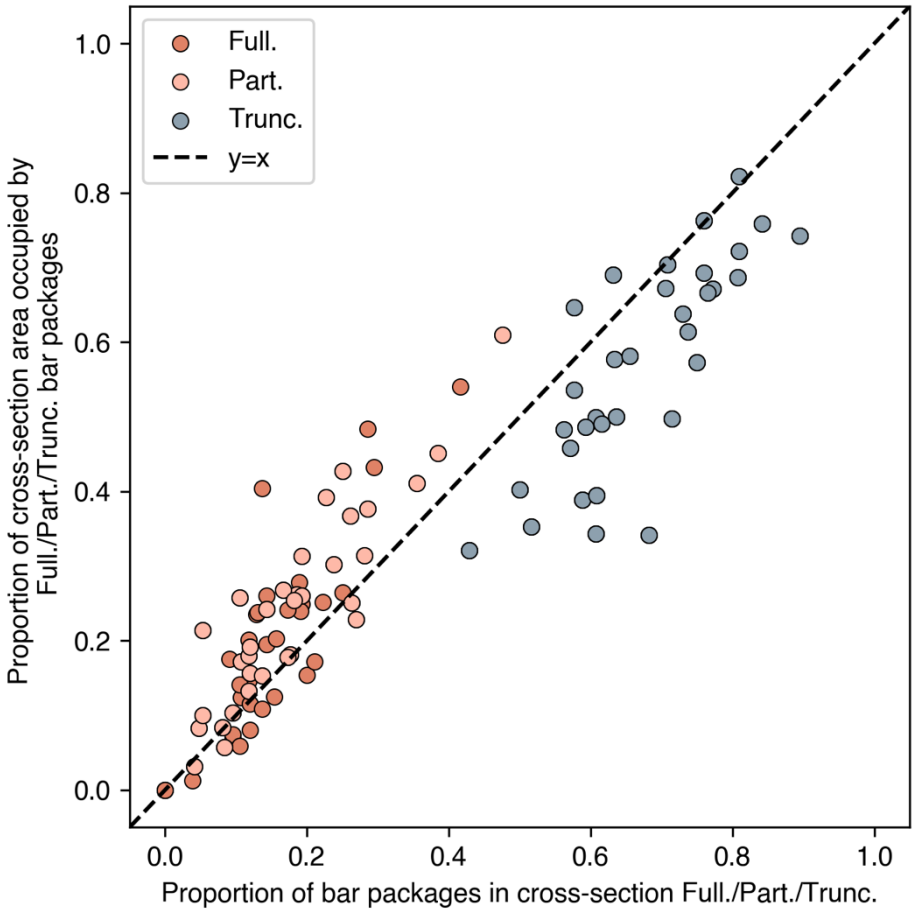

Figure S7: Comparison of preservation measurements (count-based vs. area-based) for each cross-section.

Sampling Tests

We randomly subsampled measured cross-sections to test (1) the number of random cross-sections necessary to converge on the mean bar preservation, and (2) how the flow-depth scaling factor (bar package height divided by maximum formative flow depth) in bar packages varies with sampling (see Discussion).

For the preservation test (Test 1), we drew a sample of randomly located cross-sections of sample size *n* from the distribution of mapped cross-sections. We performed this sampling 50 times with replacement. We tested this for sample sizes in which *n* is 2, 3, 4, 5, 6, 7, 8, 9, 10, 13, and 15. For each ensemble, we calculated the mean proportion of cross-section area occupied by preserved bar packages (Fully and Partially Preserved packages) and compared the distribution of means for each sample *n* to the mean proportion of cross-section area occupied by preserved bar packages in the mapped stratigraphy (red dashed line). This test highlights that after 3-4 cross-section samples, most preservation observations fall within one standard deviation of the mean bar preservation observed across all sections mapped in the system.

In Test 2 we randomly sampled the flow depth scaling factors in the distribution of mapped fully preserved bar packages that formed after model spin-up, drawing a sample of size *n* 50 times without replacement. We tested this for *n* values of 5, 10, 15, 20, 25, 30, 40, 50, 75 and 100. For each ensemble we calculated the mean flow depth scaling factor and compared the distribution of means across each sample *n* to the mean flow depth scaling factor across all preserved bar packages. When samples of 10 of more bar packages were drawn, mean flow depth scaling factors were within one standard deviation of the global average (for all mapped bar packages). When more than 30 bar packages were sampled the standard deviation within the sample sizes is minimized, and therefore these greater sample sizes provide more robust estimates of the paleohydraulic conditions in their formative systems.

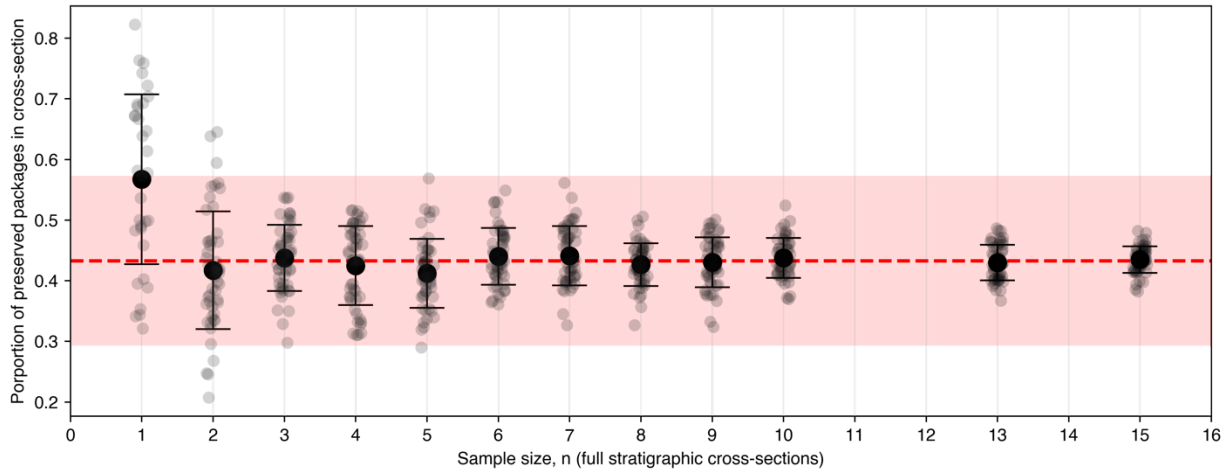

Figure S8: Results of random cross-section sub-sampling test. Circles at position 1 are the proportion of preserved bar packages at each mapped cross-section and were not included in the test. Each semi-transparent circle represents the mean proportion of preserved cross-sectional area for a drawn sub-sample of sample size n, filled black circles indicate the mean of all sub-samples drawn for each respective sample size and black error bars indicate ±1 standard deviation of the mean. Red dashed line shows the mean mapped proportion of preserved deposits in the model across all cross-sections (43%) with ±1 standard deviation (± 14%) filled above and below the global average.

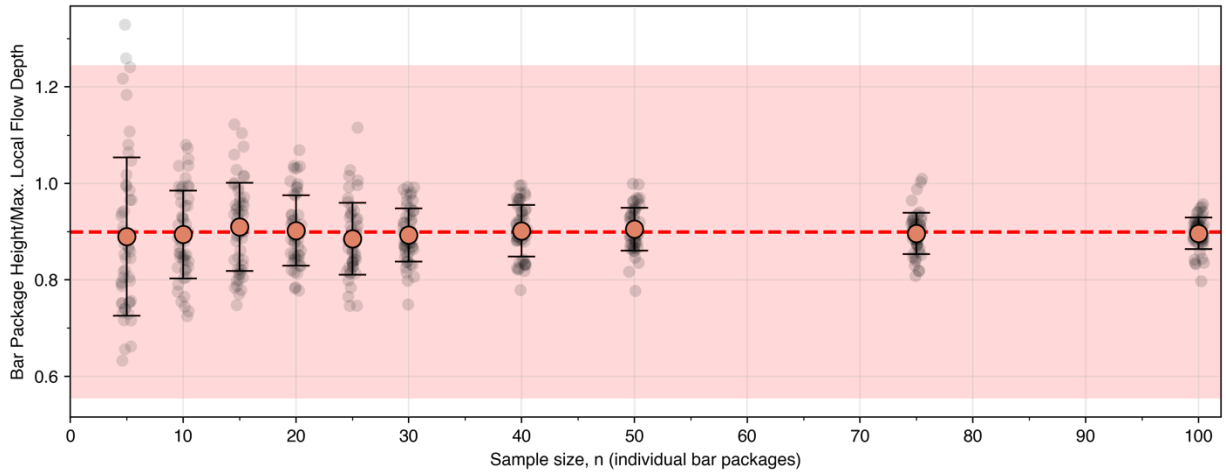

Figure S9: Results of random bar package sub-sampling test. Each semi-transparent circle represents the mean scaling factor of preserved bar packages for a drawn sub-sample of sample size n, filled orange circles indicate the mean of all sub-samples drawn for each respective sample size and black error bars indicate ±1 standard deviation of the mean. Red dashed line shows the mean flow deoth scaling factor for fully preserved deposits in the model across all cross-sections (90%) with ±1 standard deviation (± 36%) filled above and below the global average.

REFERENCES

Leary, K.C.P., and Ganti, V., 2020, Preserved Fluvial Cross Strata Record Bedform Disequilibrium Dynamics: Geophysical Research Letters, v. 47, doi:10.1029/2019GL085910.

Martin, R.L., and Jerolmack, D.J., 2013, Origin of hysteresis in bed form response to unsteady flows: Water Resources Research, v. 49, p. 1314–1333, doi:10.1002/wrcr.20093.

Myrow, P.M., Jerolmack, D.J., and Perron, J.T., 2018, Bedform Disequilibrium: Journal of Sedimentary Research, v. 88, p. 1096–1113, doi:10.2110/jsr.2018.55.

Schuurman, F., Marra, W.A., and Kleinhans, M.G., 2013, Physics-based modeling of large braided sand-bed rivers: Bar pattern formation, dynamics, and sensitivity: BRAIDED RIVER MODELING: Journal of Geophysical Research: Earth Surface, v. 118, p. 2509–2527, doi:10.1002/2013JF002896.

Shimizu, Y., Takebayashi, H., Inoue, T., Hamaki, M., Iwasaki, T., and Nabi, M., 2011, NAYS2DH Solver Manual:, https://i-ric.org/en/download/nays2dh-menual-v3/ (accessed February 2020).

Van Den Berg, J.H., and Van Gelder, A., 1993, A New Bedform Stability Diagram, with Emphasis on the Transition of Ripples to Plane Bed in Flows over Fine Sand and Silt, *in* Marzo, M. and Puigdefbregas, C. eds., Alluvial Sedimentation, Oxford, UK, Blackwell Publishing Ltd., p. 11–21, doi:10.1002/9781444303995.ch2.

Van Dijk, W.M., Van De Lageweg, W.I., and Kleinhans, M.G., 2012, Experimental meandering river with chute cutoffs: Journal of Geophysical Research: Earth Surface, v. 117, doi:10.1029/2011JF002314.